



# BUCK Type PVSC and ZETA Converter for Power Management in DC Grid

<sup>1</sup>Vijay Kr. Tiwari, <sup>2</sup>Rahul Maurya, <sup>3</sup>Atul Tiwari, <sup>4</sup>Shubham Agrahari

<sup>1</sup>Faculty, <sup>2</sup> Student, <sup>3</sup>Student, <sup>4</sup>Student

<sup>1</sup>Department of electrical engineering,

<sup>1</sup>Rajkiya Engineering College, Kannauj, India

**Abstract :** The proposed paper presents a comparative analysis of two widely used power electronic converters: Two-Loop Buck Type Converter and the ZETA Converter. Both converters play crucial roles in voltage regulation and power conditioning applications. The Two-Loop Buck Type Converter employs a dual-loop control strategy for enhanced output accuracy and stability. On the other hand, the ZETA Converter, known for its unique topology, offers advantages such as reduced input current ripple and improved efficiency. The study includes theoretical modeling, control strategy discussions, and performance evaluations for both converters under varying operating conditions. Simulation results and experimental validation are compared for proposed converter. The distributed current-mode and voltage-mode controllers are made to designed for continuous source current and voltage. The capability is especially useful for applications involving DC grids. The performance of a 48V, 177Watt converter is evaluated and compared with the results of the simulation, steady-state performance, and dynamic performance. For simulation and analysis, two programs are used: PSIM and MATLAB.

**IndexTerms -** ZETA Converter, Buck Type PVSC Converter, MIC's

## I. INTRODUCTION

Power electronics equipment has been created rapidly in the contemporary area of industrial development, introducing back DC systems in power utilization for the use of renewable energy sources such as fuel cells, wind generators and solar arrays. The technology has certainly revived the DC system in terms of power demand, with improved load management, precision, and dependability being the key problems of contemporary electricity sources. Because power electronics systems are so advanced nowadays, there is a growing need for switch-mode power converters in a variety of applications, including hybrid cars and telecommunication supply systems. With Converter's efficiency and adaptability in mind, you may effectively lower voltage levels and integrate it with a wide range of electronic equipment. The converter makes sure that your power needs are satisfied precisely and consistently whether you're using it for battery-powered applications or renewable energy systems.[1][2].

Multiple input converter (MIC) is an electronic device used to process different input sources and transform them into the desired output which shown in Fig.1. Several areas, including communications, installation, and electrical energy, use these converters. In order to deliver flexible and consistent power, the power electronics sector uses a variety of conversion schemes to regulate electricity from diverse sources, including solar panels, batteries, etc. to the grid. As a result, the energy system is more robust and sustainable.[3]. Various input converters are crucial to the processing of various signal or data stream types in signal processing. Converters function in applications like audio/video or telecommunication by combining and converting several inputs to offer smooth communication. Because of their versatility, many types of input converters can be used in complex systems that need a lot of inputs. In order to maintain the reliability and efficiency of the conversion process, the converters often use sensing technology and control techniques to modify the conversion input.

Two voltage regulation topologies are used by Buck Power Electronics: PVSC converters, and ZETA converters. The PVSC converter is a variant of the conventional Buck converter. It uses pulse width modulation, or PWM, to turn on power transistors in order to control the output voltage. The converter is widely used in applications where extremely efficient low voltage is important, such as DC-DC power supply and battery chargers. The pulsating voltage source cell (PVSC) allows output voltage regulation.

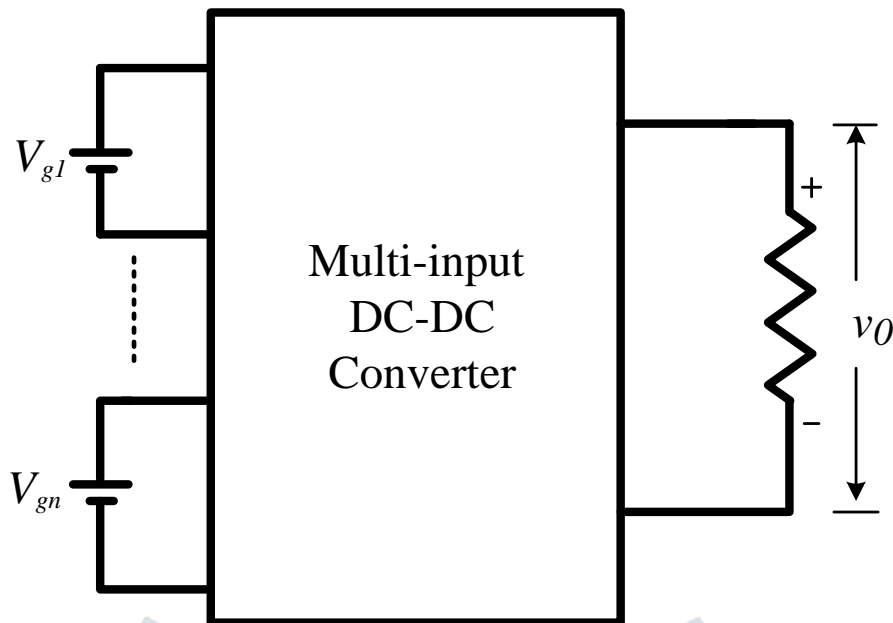


Fig.1. Diagram of n-input of DC-DC Converter

The ZETA converter is another DC-DC converter architecture that combines the qualities of Buck and Buck to ease conversion. Because it can transport electricity in both directions, it is suitable for applications such as energy storage.[4][5]. To guarantee efficiency and dependability, various DC-DC converter connections in electrical equipment must perform properly. The piece discusses offers advantages like reduced input current ripple and increased efficiency because of its unique topology. The work includes theoretical modelling, discussions of control techniques, and performance evaluations for both converters under various operating conditions. Researchers and engineers can choose the most appropriate solutions for controlling particular energy types by using simulation results and experimental validation to highlight the capabilities, benefits, and limitations of each converter.[6][7]. Similar to the SEPIC DC/DC converter design, the ZETA converter gives a positive output value from an input voltage that varies above and below the output. The ZETA converter also requires a series capacitor, also referred to as a flying capacitor, and two inductors. The ZETA converter is designed using a buck controller that powers a high-side PMOS transistor, as opposed to the SEPIC converter, which is designed with a typical boost converter. The ZETA converter is an additional option for regulating an input-power source, such as a low-cost plug-in converter. Using a connected inductor can reduce the amount of board space required. The article describes how to create a ZETA converter using a connected inductor that operates in continuous-conduction mode (CCM). Meeting the rising power demand is the main issue with modern dc systems of distribution, such as found in telecom and automotive power supply systems and to less the demand on the built-in battery, which serves as the main energy source. It is possible by connecting other power sources in parallel with the current battery source. Renewable energy sources like fuel cell (FC) storage power or photovoltaic (PV) power can be used as the additional power source.[5]-[9]. Power electronics equipment has been created rapidly in the current era of industrial development, bringing back the use of clean DC power systems in power utilization. Energy sources such as fuel cells, wind generators, solar arrays, etc.

Power electronics equipment has grown in popularity over High-switching-frequency dc-dc converters become more common in small-sized power electronics equipment in recent years. In order to optimize energy consumption from various sources such as fuel cells, batteries, wind and solar energy, many power electronics dc-dc converters have been suggested in the research.[8]. In the field of power electronics, the design and analysis of multi-input DC-DC converters are essential because they provide solutions for a variety of applications where it's necessary to connect various power sources efficiently. The converters are vital parts of electric cars, renewable energy systems, and many other power management systems. An overview of the primary components involved in the design and analysis of multi-input DC-DC converters is given. The requirement for adaptable and effective energy conversion in contemporary power systems is growing. Multi-input DC-DC converters meet demand by allowing the integration of many power sources, such as solar panels, batteries, and traditional power supply. They provide smooth energy management, increasing the overall reliability and efficiency of the system.[10][11].

## II. PROPOSED MULTI INPUT CONVERTER

The schematic design of two-input Buck type PVSC and ZETA converter is illustrated in Fig.2, consists of two power sources ( $V_{g1}$  and  $V_{g2}$ ), two switching devices, and four energy storage units, making it a fourth-order system. In the proposed topology, the buck-type PVSC does not create a mesh with the output when it is connected in series with Zeta converter's current buffer the Zeta Converter's sink. The input source the buck-type PVSC can only supply power to the energy buffer rather than the load directly. Otherwise, it can only supply power to the load when the primary PWM input source of converter does so simultaneously.[12].

The PWM gating signals and Off- Time sampling process shown in Fig.3 and the mode of operation of converter is given in below Table.1.

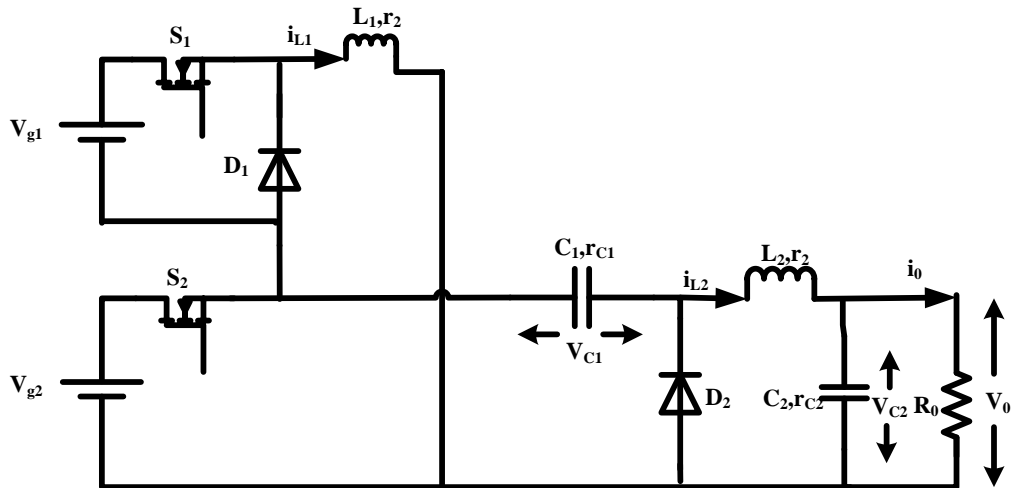


Fig.2. Proposed MIC

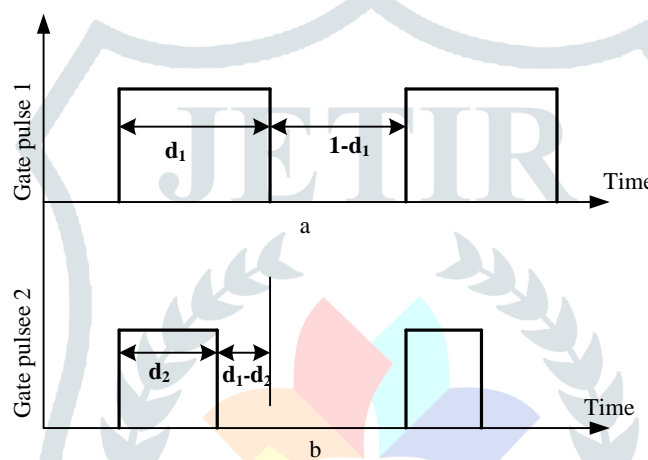


Fig.3. PWM gating signals and Off- Time sampling process

Table.1. SWITCH AND DIODE ON/OFF CONDITION DURING DIFFERENT MODES

MODE	SWITCH(S <sub>1</sub> )	SWITCH(S <sub>2</sub> )	DIODE(D <sub>1</sub> )	DIODE(D <sub>2</sub> )
Mode-1	ON	ON	OFF	OFF
Mode-2	ON	OFF	OFF	ON
Mode-3	OFF	OFF	ON	ON

### III. ANALYSIS OF MULTI- INPUT CONVERTER

The proposed converter has four energy storage units, resulting in a fourth-order system. The converter has two capacitors and two inductors linked. The parasitic resistance of inductors and capacitors is ignored. For the state-space modelling approach is carefully thought about/believed, and separate-time modelling is to frame a digital controller. In proposed paper, the  $d_1 > d_2$  is carefully studied with trailing-edge off-time sampling. As the voltage on both sources is not as important in the study as the voltage generated by the DC grid, it is preferable to use the converter's boosting action to increase the voltage on the load side.[13][14].

If the system is linear and time invariant, a set of matrix-form state equations that explain the system dynamics for each mode of operation can be derived below:

$$\dot{x} = A_k x + B_k u \tag{1}$$

$$Y = E_k x + F_k u \tag{2}$$

Where,

$$[X] = [I_{L1} \quad I_{L2} \quad V_{C1} \quad V_{C2}]^T$$

$$U = [V_{g1} \quad V_{g2}]^T$$

where for cycles 1, 2, and 3,  $k=1, 2,$  and  $3,$  accordingly. system matrix =  $A_k,$  feed-forward matrix =  $F_k,$  input matrix =  $B_k,$  output matrix =  $E_k.$

From eq.1 state space matrices in the relevant mode can be expressed as,

**Mode-1 [0 < t < d<sub>2</sub>T<sub>s</sub>] :-**

The switches S1 and S2 are ON while diodes D1 and D2 are OFF, the source energy inductor L1 and L2 are changing linearly by voltage V<sub>g1</sub> and V<sub>g2</sub> respectively having capacitor C1 and C2 maintain the load voltage.

The state-variable matrix for mode-1 obtained in the circuit illustrated in Fig.4 by using Kirchhoff's voltage and current law eq.3-6.

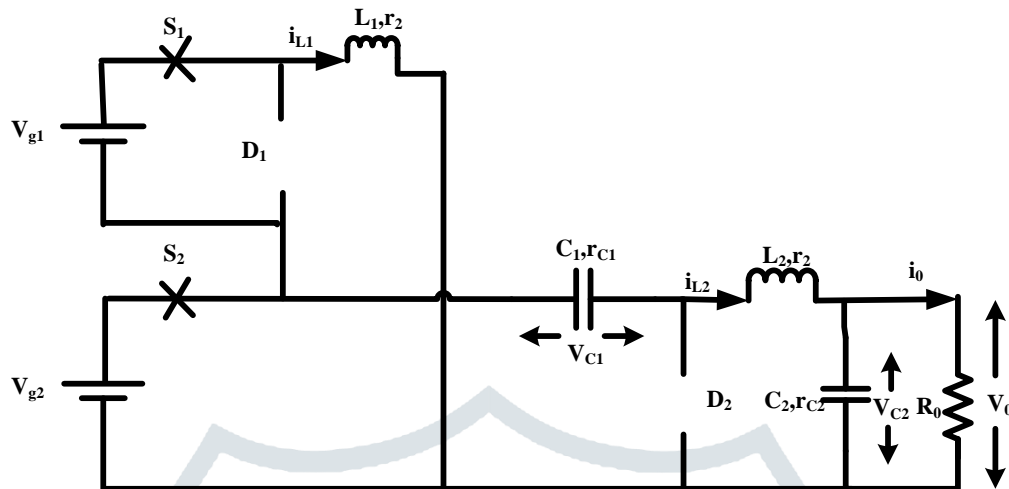


Fig.4. Equivalent circuit diagram of mode-1

State space matrix of mode-1 is :-

$$A_1 = \begin{bmatrix} -\left(\frac{r_{L1}}{L_1}\right) & 0 & 0 & 0 \\ 0 & \frac{-1}{L_2} \left( r_{C1} + r_{L2} + \frac{R_0 r_{C2}}{r_{C1} + R_0} \right) & -\left(\frac{1}{L_2}\right) & \frac{-R_0}{L_2(r_{C2} + R_0)} \\ 0 & \frac{1}{C_1} & 0 & 0 \\ 0 & \frac{R_0}{C_2(r_{C2} + R_0)} & 0 & \frac{-1}{C_2(r_{C2} + R_0)} \end{bmatrix} \tag{3}$$

The mode-1 input matrix B<sub>1</sub> can be written as:-

$$B_1 = \begin{bmatrix} \frac{1}{L_1} & 0 & 0 & 0 \\ \frac{1}{L_1} & \frac{1}{L_2} & 0 & 0 \end{bmatrix}^T \tag{4}$$

Input current matrix P<sub>1</sub> for mode-1 is:-

$$P_1 = \begin{bmatrix} 1 & 0 & 0 & 0 \\ 1 & 1 & 0 & 0 \end{bmatrix} \tag{5}$$

$$F_1 = F_2 = F_3 = [0] \tag{10}$$

**Mode-2 [d<sub>2</sub>T<sub>s</sub> < t < (d<sub>1</sub>-d<sub>2</sub>)T<sub>s</sub>] :-**

The devices S1 and D2 are ON while S2 and D1 are OFF, inductor L1 current will decreases and in L2 current will increases.

The state-variable matrix for mode-2 obtained in the circuit illustrated in Fig.5 by using Kirchhoff's voltage and current law eq.7-9.

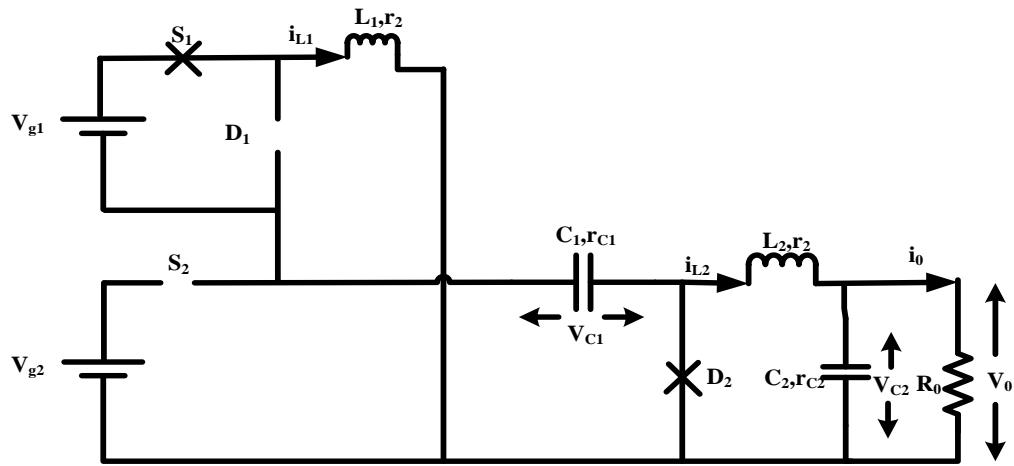


Fig.5. Equivalent circuit diagram of mode-2

State space matrix of mode-2 is :-

$$A_2 = \begin{bmatrix} -\frac{1}{L_1}(r_{L1} + r_{C1}) & 0 & \frac{1}{L_1} & 0 \\ 0 & -\frac{1}{L_2}\left(r_{L2} + \frac{R_0 r_{C2}}{r_{C2} + R_0}\right) & 0 & \frac{-R_0}{L_2(r_{C2} + R_0)} \\ -\left(\frac{1}{C_1}\right) & 0 & 0 & 0 \\ 0 & \frac{R_0}{C_2(r_{C2} + R_0)} & 0 & \frac{-1}{C_2(r_{C2} + R_0)} \end{bmatrix} \tag{7}$$

The mode-2 input matrix B<sub>2</sub> can be written as:-

$$B_2 = \begin{bmatrix} \frac{1}{L_1} & 0 & 0 & 0 \\ 0 & 0 & 0 & 0 \end{bmatrix}^T \tag{8}$$

Input current matrix P<sub>2</sub> for mode-2 is:-

$$P_2 = \begin{bmatrix} 1 & 0 & 0 & 0 \\ 0 & 0 & 0 & 0 \end{bmatrix} \tag{9}$$

**Mode-3 [(d<sub>1</sub>-d<sub>2</sub>)Ts < t < (1-d<sub>1</sub>)] :-**

The Switches S<sub>1</sub> and S<sub>2</sub> are OFF while diodes diode D<sub>1</sub> and D<sub>2</sub> are ON. Since the power of load resistance are managed by the sources.

The state-variable matrix for mode-3 obtained in the circuit illustrated in Fig.6 by using Kirchhoff's voltage and current law eq.10-13.

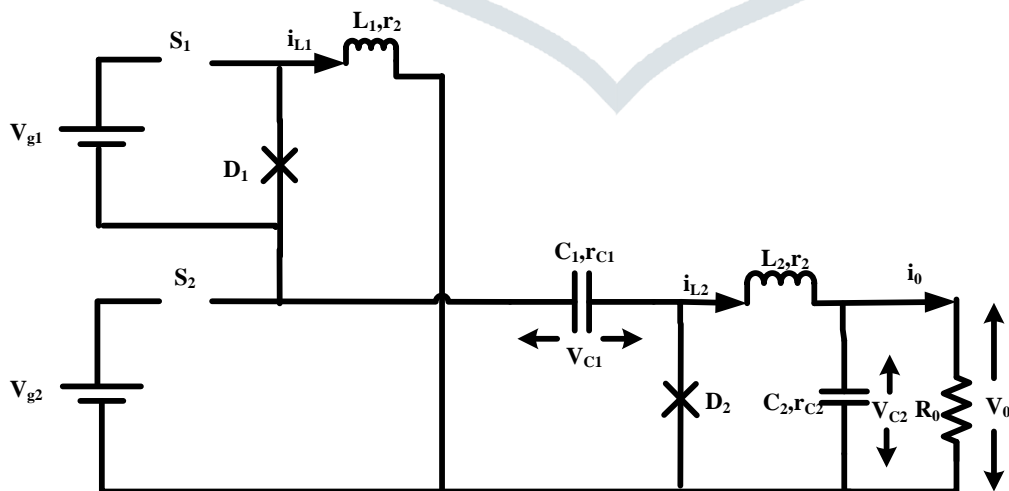


Fig.6. Equivalent circuit diagram of mode-3

State space matrix of mode-3:-

$$A_3 = \begin{bmatrix} -\frac{1}{L_1}(r_{L1} + r_{C1}) & 0 & \frac{1}{L_1} & 0 \\ 0 & \frac{-1}{L_2}\left(r_{L2} + \frac{R_0 r_{C2}}{r_{C2} + R_0}\right) & 0 & \frac{-R_0}{L_2(r_{C2} + R_0)} \\ -\left(\frac{1}{C_1}\right) & 0 & 0 & 0 \\ 0 & \frac{R}{C_2(r_{C2} + R_0)} & 0 & \frac{-1}{C_2(r_{C2} + R_0)} \end{bmatrix} \quad (10)$$

The mode-3 input matrix  $B_3$  can be written as:-

$$B_3 = \begin{bmatrix} 0 & 0 & 0 & 0 \\ 0 & 0 & 0 & 0 \end{bmatrix}^T \quad (11)$$

Input current matrix  $P_3$  for mode-3 is

$$P_3 = \begin{bmatrix} 0 & 0 & 0 & 0 \\ 0 & 0 & 0 & 0 \end{bmatrix} \quad (12)$$

Output matrix  $E_1 = E_2 = E_3$  can be expressed as:-

$$E_1 = E_2 = E_3 = \begin{bmatrix} 0 & \frac{R_0 r_{C2}}{r_{C2} + R_0} & 0 & \frac{R_0}{r_{C2} + R_0} \end{bmatrix} \quad (13)$$

#### IV. VOLT SECOND BALANCE EQUATION

According to volt second balance, the average value of voltage across on inductor is zero in a switching cycle.

For the Inductor  $L_1$ :

$$(V_{g1} + V_{g2})d_2 + (V_{g1} + V_{c1})(d_1 - d_2) + V_{c1}(1 - d_1) = 0$$

$$V_{c1} = \frac{V_{g2}d_2 + V_{g1}d_1}{(d_2 - 1)} \quad (14)$$

For the inductor  $L_2$ :

$$(V_{g2} - V_{c1} - V_{c2})d_2 + (-V_{c2})(d_1 - d_2) + (-V_{c2})(1 - d_1) = 0$$

$$V_0 = V_{g2} \cdot d_2 - V_{c1} \cdot d_2 \quad (15)$$

From equation (14) and (15):

$$V_0 = \frac{V_{g2}d_2 + V_{g1}d_1d_2}{1 - d_2} \quad (16)$$

#### V. DISCRETE TIME MODELLING

Discrete-time modeling of the converter in detail has been done [15]. The suggested two input converter is modeled in discrete time, and the final equation are given below [16]. Four intervals are taken from one full sample period ( $[(n-1)T_s]$  to  $[nT_s]$ ). Below is list of each time interval:

$$\text{Interval -1: } (n-1)T_s < t < [(n-1)T_s + t_d - d_2T_s] \quad (17)$$

$$\text{Interval -2: } [(n-1)T_s + t_d - d_2T_s] < t < [(n-1)T_s + t_d] \quad (18)$$

$$\text{Interval -3: } [(n-1)T_s + t_d] < t < [(n-1)T_s + t_d + (d_1 - d_2)T_s] \quad (19)$$

$$\text{Interval -4: } [(n-1)T_s + t_d + d_1 - d_2)T_s] < t < [nT_s] \quad (20)$$

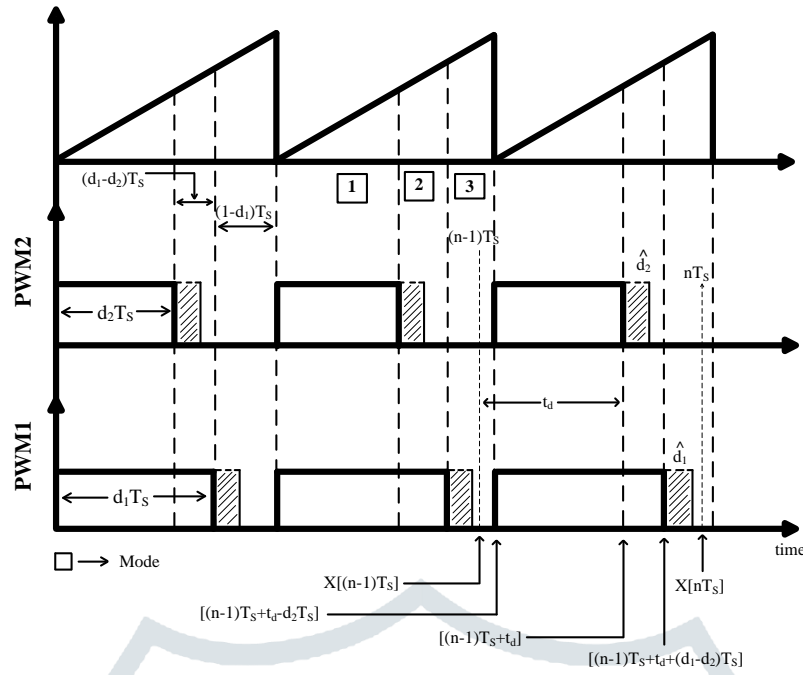


Fig.7. Waveforms for trailing-edge OFF-Time sampling.

A small-signal model in discrete-time domain of converter under analysis is shown below.

$$\hat{X}[nT_s] = \phi \hat{X}[(n-1)T_s] + \gamma_2 \hat{d}_1 [(n-1)T_s] + \gamma_1 \hat{d}_2 [(n-1)T_s] \tag{21}$$

Where,

$$\phi = e^{AT_s}$$

$$\gamma_1 = K_1 T_s e^{A_1(d_1-d_2)T_s + A_2[T_s-t_d-d_2T_s]}$$

$$\gamma_2 = K_2 T_s e^{A_3[T_s-t_d-d_1T_s+d_2T_s]}$$

Table 2. DESIGN EXPRESSION AND PARAMETER VALUES

Design Parameter	Expression	Value of Parameters
L <sub>1</sub>	$\frac{(V_{g1} + V_{g2}) * d_1}{f_s * (\Delta i_{L1})}$	100μH
L <sub>2</sub>	$\frac{V_0 * (1 - d_1)}{f_s * \Delta i_{L2}}$	700μH
C <sub>1</sub>	$\frac{i_{L2} * d_1}{f_s * (\Delta v_{c1})}$	27μF
C <sub>2</sub>	$\frac{(i_{L2} - i_0) * d_1}{f_s * (\Delta v_{c2})}$	27μF

Table 3. CONVERTER SPECIFICATION

Parameters	Numerical Value
Load voltage	V <sub>o</sub> = 48 V
Power rating	P ≈ 177 W
DC source voltage	V <sub>g1</sub> =24 V, V <sub>g2</sub> =36 V
Voltage ripple	≤5%
Current ripple	≤10%
Switching frequency	50 kHz

VI. SIMULATION STUDIES AND EXPERIMENTAL RESULT

$$G_{t1} = \frac{0.2598Z^2 - 0.1215Z + 0.01228}{Z^4 - 3.535Z^3 + 4.839Z^2 - 3.048Z + 0.7474} \tag{22}$$

$$G_{t2} = \frac{14.21Z^3 - 29.43Z^2 + 18.2Z - 2.326}{Z^4 - 3.535Z^3 + 4.839Z^2 - 3.048Z + 0.7474} \tag{23}$$

$$G_{t3} = \begin{matrix} \text{From input to output} \\ 1-: \frac{3.934Z^3 - 10.38Z^2 + 9.64Z - 3.194}{Z^4 - 3.535Z^3 + 4.839Z^2 - 3.048Z + 0.7474} \\ 2-: \frac{3.934Z^3 - 9.006Z^2 + 8.336Z - 2.792}{Z^4 - 3.535Z^3 + 4.839Z^2 - 3.048Z + 0.7474} \end{matrix} \tag{24}$$

$$G_{t4} = \begin{matrix} \text{From input to output} \\ 1-: \frac{10.95Z^3 - 28.18Z^2 + 25.83Z - 8.554}{Z^4 - 3.535Z^3 + 4.839Z^2 - 3.048Z + 0.7474} \\ 2-: \frac{18.63Z^3 - 50.35Z^2 + 47.4Z - 15.63}{Z^4 - 3.535Z^3 + 4.839Z^2 - 3.048Z + 0.7474} \end{matrix} \tag{25}$$

The pole zero plot of the transfer function is illustrated in Fig.8. The pole-zero diagram clearly shows that the all zeros and poles are inside the unit circle, indicating that the converter system belongs to the non-minimum phase system and the converter is stable.

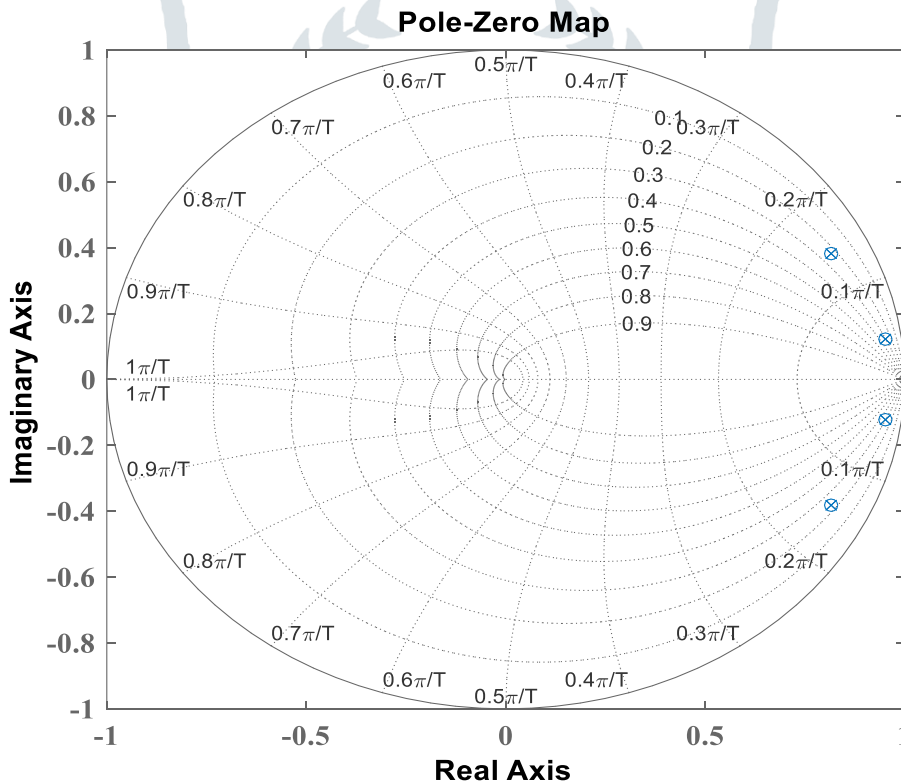


Fig.8. Pole Zero plot of the transfer function (G)

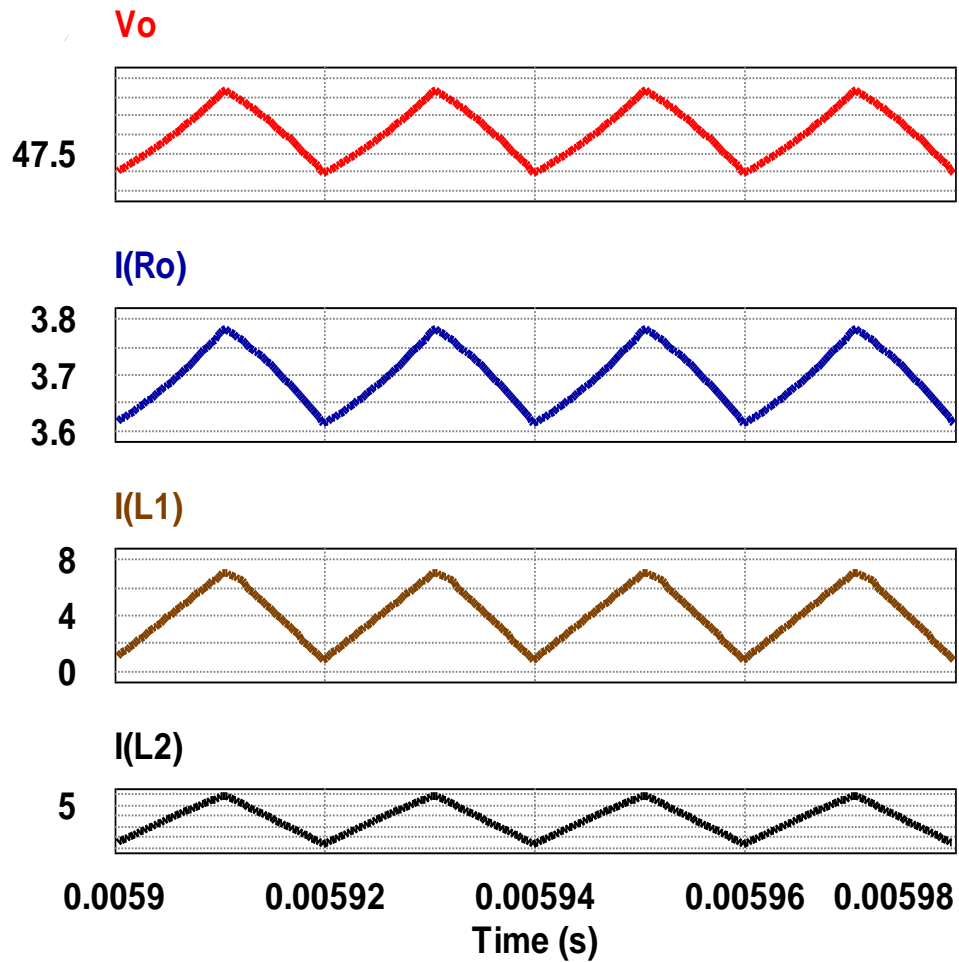


Fig.9. Study state waveform of inductor and load current

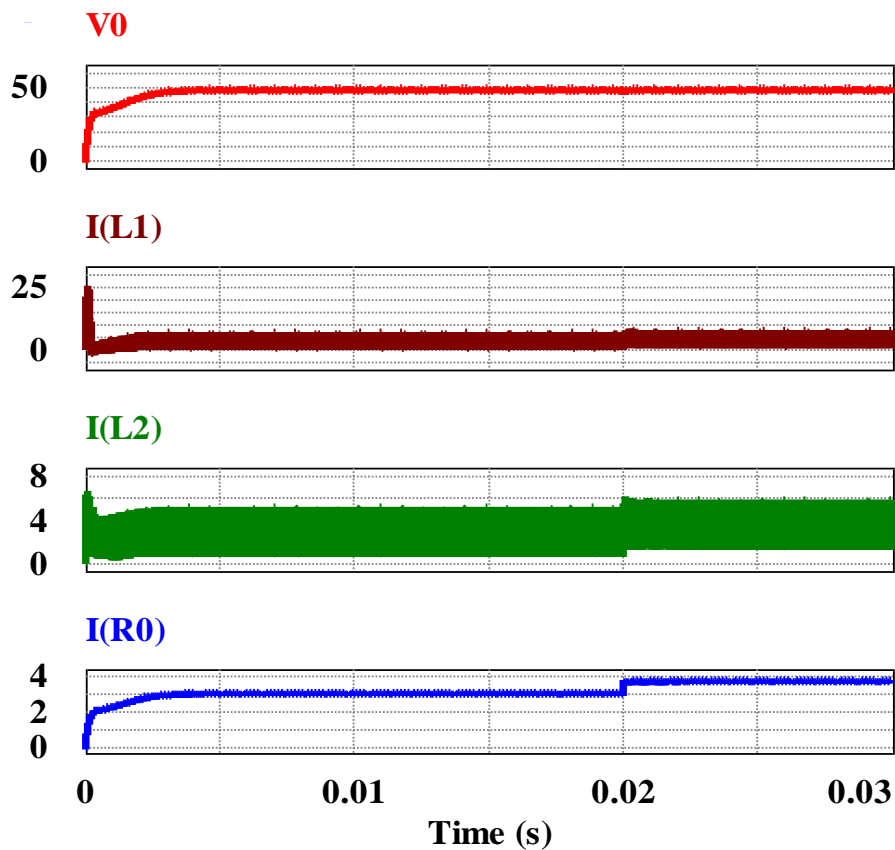


Fig.10. Simulation waveform for close loop

The close loop simulation results are shown in Fig.10. After giving disturbances at 20milliseconds, the load voltage ( $V_0$ ) waveform remains constant, while the load current waveform increases

## VII. CONCLUSION

A new Buck-based two-input dc-dc converter topologies for dc grid applications for power control. After analysing the mode of operation, decoupled control loops were created to balance the load demand between the two input sources, Discrete-time modelling was performed for each mode of operation. The experiments showed that power control on the input sources can be performed with easily and has no impact with the dc-grid's ability to load. The results of simulations and experiments nearly matched theoretical research.

## REFERENCES

- [1] M. Veerachary, "Two-Loop Controlled Buck–SEPIC Converter for Input Source Power Management," in *IEEE Transactions on Industrial Electronics*, vol. 59, no. 11, pp. 4075–4087, Nov. 2012.
- [2] B. Zhu, Hu. Hui, H. Wang, Y. Li, A multi-input-port bidirectional DC/DC converter for DC microgrid energy storage system applications. *Energies* 13(11), 2810 (2020)
- [3] Li, Y., Ruan, X., Yang, D., Liu, F. and Chi, K.T. "Synthesis of multiple-input DC/DC converters" *IEEE Transactions on Power Electronics*, 25(9), pp.2372-2385, 2010.
- [4] Eng Vuthchhay and Chanin Bunlaksanansorn, "Dynamic modeling of a zeta converter with state-space averaging technique," *Proc. 5th Int. Conf. Electrical Engineering/Electronics, Computer, Telecommunications and Information Technology (ECTI-CON) 2008*, Vol. 2.
- [5] M. Ghavaminejad, E. Afei and M. Meghdadi, "Double-Input/Double-Output Buck- Zeta Converter," 2021 29th Iranian Conference on Electrical Engineering (ICEE), Tehran, Iran, Islamic Republic of, 2021.
- [6] Z. Rehman, I. Al-bahadly, and S. Mukhopadhyay, "Multi-input DC – DC converters in renewable energy applications – An overview," *Renew. Sustain. Energy Rev.*, vol. 41, pp. 521– 539, 2015.
- [7] C. Yao, X. Ruan, X. Wang, and C. K. Tse, "Isolated Buck–Boost dc/dc converters suitable for wide input-voltage range," *IEEE Trans. Power Electron.*, vol. 26, no. 9, pp. 2599–2613, Sep. 2011.
- [8] Y.C. Liu, Y.M. Chen, A systematic approach to synthesizing mul-tiple-input dc- dconverter. *IEEE Trans. Power Electron.* 24(1), 116–127 (2009).
- [9] Z. Wang, Q. Luo, Y. Wei, D. Mou, X. Lu, P. Sun, Topology analysis and review of three-port DC/DC converters. *IEEE Transactions on Power Electronics* 35, 11783– 11800 (2020).
- [10] Y. Jeong, J.-D. Park, R. Rorrer, K.-W. Kim, B.-H. Lee. A novel multi-input and single- output DC/DC converter for small unmanned aerial vehicle, in 2020 *IEEE Applied Power Electronics Conference and Exposition (APEC)*. IEEE, pp. 1302–1308 (2020).
- [11] B. Zhu, Hu. Hui, H. Wang, Y. Li, A multi-input-port bidirectional DC/DC converter for DC microgrid energy storage system appli- cations. *Energies* 13(11), 2810 (2020).
- [12] Z. Shan, X. Ding, J. Jatskevich, K. TseChi, Synthesis of multi- input multi-output DC/DC converters without energy buffer stages. *IEEE Trans. Circuits Syst. II Express Briefs* 68, 712–716 (2020).
- [13] Wai, R.J., Duan, R.Y. and Jheng, K.H., "High-efficiency bidirectional dc–dc converter with high-voltage gain," *IET Power Electronics*, 5(2), pp.173-184, 2012
- [14] P. Yang, C. K. Tse, J. Xu, and G. Zhou, "Synthesis and Analysis of Double-Input Single-Output DC/DC Converters," *IEEE Trans. Ind. Electron.*, 62(10), pp. 6284– 6295, 2015.
- [15] M. Veerachay, Vijay Kumar Tewari, Anandh. N. "Two input boosting dc-dc converter for dc grid application", *IEEE conference on Green computing communication and conservation of energy*, vol. 54, pp. 574 579, 2013.
- [16] Maksimovic, Dragan & Zane, Regan. (2007). Small-Signal Discrete-Time Modeling of Digitally Controlled PWM Converters. *Power Electronics, IEEE Transactions on*. 22. 2552 - 2556. 10.1109/TPEL.2007.909776.
- [17] Veerachary M, Tiwari VK (2014) Power management in dc-grid through two input dc-dc converter. *Eighteenth National Power Systems Conference (NPSC)*. IEEE, pp 1–6
- [18] Tewari, V.K., Verma, A. Two-Loop Controlled Quasi Multiple Input DC–DC Converter for Load Voltage and Source Current Management. *Trans. Electr. Electron. Mater.* 23, 72–80 (2022).
- [19] Veerachary M, Tewari VK, Anandh N (2013) Two-input boosting dc-dc converter for dc-grid applications. *International conference on green computing, communication and conservation of energy (ICGCE)*. IEEE, pp 574–579
- [20] Tewari, V.K., Verma, A. Design and Application of Double-Gate MOSFET in Two Loops Controlled Multi-Input DC–DC Converter. *Silicon* 14, 7321–7333 (2022). <https://doi.org/10.1007/s12633-021-01469-7>
- [21] Singh, J., Verma, A., Tewari, V.K. et al. Design and Parametric Analysis of GaN on Silicon High Electron Mobility Transistor for RF Performance Enhancement. *Silicon* 14, 6311–6319 (2022). <https://doi.org/10.1007/s12633-021-01419-3>